Available online at www.sciencedirect.com
ScienceDirect
International Journal of Solids and Structures 45 (2008) 3122–3137
INTERNATIONAL JOURNAL OF SOLIDS AND STRUCTURES
www.elsevier.com/locate/ijsolstr

The capillary force in micro- and nano-indentation with different indenter shapes

S.H. Chen [a,*], A.K. Soh [b,1]

[a] LNM, Institute of Mechanics, Chinese Academy of Sciences, No. 15, BeiSiHuan Xilu, Beijing 100080, China
[b] Department of Mechanical Engineering, The University of Hong Kong, Hong Kong

Received 7 August 2007; received in revised form 15 January 2008
Available online 26 January 2008

Abstract

The influence of the indenter shapes and various parameters on the magnitude of the capillary force is studied on the basis of models describing the wet adhesion of indenters and substrates joined by liquid bridges. In the former, we consider several shapes, such as conical, spherical and truncated conical one with a spherical end. In the latter, the effects of the contact angle, the radius of the wetting circle, the volume of the liquid bridge, the environmental humidity, the gap between the indenter and the substrate, the conical angle, the radius of the spherical indenter, the opening angle of the spherical end in the truncated conical indenter are included. The meniscus of the bridge is described using a circular approximation, which is reasonable under some conditions. Different dependences of the capillary force on the indenter shapes and the geometric parameters are observed. The results can be applicable to the micro- and nano-indentation experiments. It shows that the measured hardness is underestimated due to the effect of the capillary force.

Keywords: Capillary force; Micro- and nano-indentation; Indenter shape; Humidity

1. Introduction

The permanent adhesion arises from various types of interfacial forces, such as capillary, electrostatic and van der Waals forces. Among these forces, the capillary force is dominant in the nano-scale contact.

Capillary force exists everywhere under real-life conditions. A powder absorbs moisture from the surroundings because of the adsorption of water vapors at the particle surfaces and the capillary condensation of this water in the pores of the material (Tselishchev and Val'tsifer, 2003). Capillary force is also very important in MEMS. During the fabrication of micro- or nano-scale components on silicon substrates, the oxidized polysilicon surface is hydrophilic and the capillary force formed between the structure

* Corresponding author. Tel.: +86 10 82543960; fax: +86 10 82543977.
E-mail addresses: chenshaohua72@hotmail.com (S.H. Chen), aksoh@hkucc.hku.hk (A.K. Soh).
[1] Tel.: +852 28598061.

0020-7683/$ - see front matter © 2008 Elsevier Ltd. All rights reserved.
doi:10.1016/j.ijsolstr.2008.01.014

and substrate is sufficiently strong to collapse the microstructure, which is called release-related adhesion. Several engineering approaches to minimize release-related adhesion have been investigated (Maboudian, 1998a; Maboudian et al., 2000) and self-assembled monolayer has been widely focused because it converts the surface to be hydrophobic (Maboudian, 1998b). In micro-manipulation, the influence of gravitational force is extremely small compared to adhesion force, the capillary force is large enough to detach an adhered particle if the liquid has volume sufficiently smaller than that of the particle (Tanikawa et al., 1998).

In biological attachment systems, dry adhesion is adopted by geckos, jumping spiders, etc. (For examples, Autumn et al., 2002; Kesel et al., 2003). These animals have achieved superior attachment ability through the van der Waals force. Animals like beetles and ants have not evolved the same attachment terminals as geckos (For examples, Eisner and Aneshansley, 2000; Federle et al., 2004). They resort to another strategy, which is based on wet adhesion. When they attach to surfaces, some secretory fluid is produced and delivered to the bottom of the attachment pads. Experiments have verified that the capillary force is very important to their ability to adhere on surfaces (Dixon et al., 1990).

Different models and experiments have been established to investigate the wet adhesion between objects with different shapes and a solid plane. For examples, Orr et al. (1975) considered a liquid bridge between a sphere and a plate and obtained analytical expressions for the bridge profile in terms of elliptic integrals. Fortes (1982) studied the capillary force with axisymmetric liquid bridge between two parallel plates. Tselishchev and Val'tsifer (2003) investigated the influence of the particle dimensions and type of interparticle contact on the magnitude of the capillary forces between the powder particles. Yoon et al. (2003) did nano-contact experiments and studied the effect of the capillary force in various relative humidity. Obata et al. (2004) proposed a micro-manipulation method because the capillary force could be controlled by regulation of the volume of the liquid bridge. In order to decrease the wet adhesion, effective surface treatments are required. Providing a stable hydrophobic surface is one example to decrease the formation of water layers on the surface, thereby decreasing the capillary forces (Maboudian and Howe, 1997; Yoon et al., 2003). Pakarinen et al. (2005) numerically calculated the exact meniscus profile from the Kelvin equation and found that a circular meniscus profile would give correct results in most cases. In order to increase the wet adhesion, size reduction and long effective interaction range are helpful (Qian and Gao, 2006).

Almost in all of the above studies on capillary forces, the gap between the two objects are not less than zero, i.e., $D \geqslant 0$. It is well known that the environmental humidity should have significant effects on the results of micro- and nano-indentation, which are mainly used to measure the materials' hardness. In order to get the hardness of materials, continuous stiffness method is often used to obtain the load–depth relation, from which the hardness of materials can be calculated. The micro- and nano-indentation hardness of bulk materials and film-substrate systems has been studied by many researchers (For examples, Ma and Clarke, 1995; McElhaney et al., 1998; Nix and Gao, 1998; Huang et al., 2000; Chen et al., 2004a,b) and the size effect in the indentation experiments are mainly focused in these years, i.e., the indentation hardness increasing with a decreasing indentation depth, when the indentation depth is less than several tens micrometers. Only the load acted externally is considered in studying the indentation hardness. Nobody considers the effect of the capillary force. Furthermore, the indenter should penetrate into the measured object continuously, so that the gap considered in the above literatures on capillary force should be negative in the indentation models. Some questions will be proposed obviously. Are there any different phenomena between $D \geqslant 0$ and $D < 0$? What is the effect of humidity on the capillary force when $D < 0$? How does the rounded indenter tip influence the capillary force? What is the effect of capillary force on measured hardness? All these questions bestir us to repeat the present research in details, though some of the models in the present paper have already been studied before (For examples, Yoon et al., 2003; Tselishchev and Val'tsifer, 2003; Pakarinen et al., 2005).

In this paper, the methods for calculating the capillary force of different models are presented. The effects of the indenter shape, the radius of the wetting circles, the distance between the indenter and the substrate, the volume of the liquid bridge and the relative humidity on the magnitude of the capillary force are mainly investigated in details. The effects of the capillary force on the indentation hardness in micro- and nano-indentation experiments are discussed.

2. Circular assumption and conception of relative humidity

The capillary force for a sphere, a cone and a truncated cone in wet adhesive contact with a solid plane will be studied to simulate the indentation experiments with different indenter shapes. The liquid between the indenter and the substrate is assumed to be water due to the environmental humidity. The surface tension $\Delta\gamma$ is assumed to be a constant though the confinement of a liquid or even the presence of a solid surface may change the effective surface tension of the liquid at a nano-scale, i.e., $\Delta\gamma = 0.072$ N/m. The liquid bridge surface is curved because of an interaction of the liquid molecules with each other. We assume the meniscus of the bridge to be a circular arc according to Pakarinen et al. (2005) and Farshchi-Tabrizi et al. (2006). Thus the contact angles θ_1 and θ_2 of the liquid on the indenter and the substrate can be described as θ, i.e.,

$$\theta_1 = \theta_2 = \theta \tag{1}$$

The environmental humidity is described by the relative vapor pressure P/P_0, where P is the actual vapor pressure and P_0 is the saturation vapor pressure of a reference planar liquid surface, which can be calculated using the Kelvin equation

$$\frac{P}{P_0} = \exp\left[-\frac{\Delta\gamma V_m}{R_G T}\left(\frac{1}{r} - \frac{1}{l}\right)\right] \tag{2}$$

in which $R_G = 8.268$ J/(K mol) is the gas constant, $T = 298$ K is the temperature, $V_m = 18 \times 10^{-6}$ m^3/mol and $\Delta\gamma = 0.072$ N/m are the molar volume and surface tension of water, respectively. r and l describe two principal radii of curvature.

3. Wet adhesion between a conical indenter and a solid plane

Fig. 1a and b shows a model for the analysis of wet adhesion between a conical indenter and a solid substrate, where b is the radius of the circle of the liquid bridge wetting the cones, α is half of the cone angle, $\theta_1 = \theta_2 = \theta$ is the contact angle, D is the gap between the indenter and the substrate, the curvature radii r and l of the liquid bridge are also shown in the figures.

The magnitude of the capillary force F_c depends on two components. The first one is determined by the surface tension of the liquid $\Delta\gamma$. The second one is owing to the pressure difference Δp inside and outside the meniscus. Since the effect of gravity is neglected in our study, Δp is a constant within the meniscus.

(1) For the case of $D \geqslant 0$, the capillary force is

$$F_c = -\pi b^2 \Delta p + 2\pi b \Delta\gamma \cos(\alpha - \theta) \tag{3}$$

and the pressure difference is described by the Laplace equation,

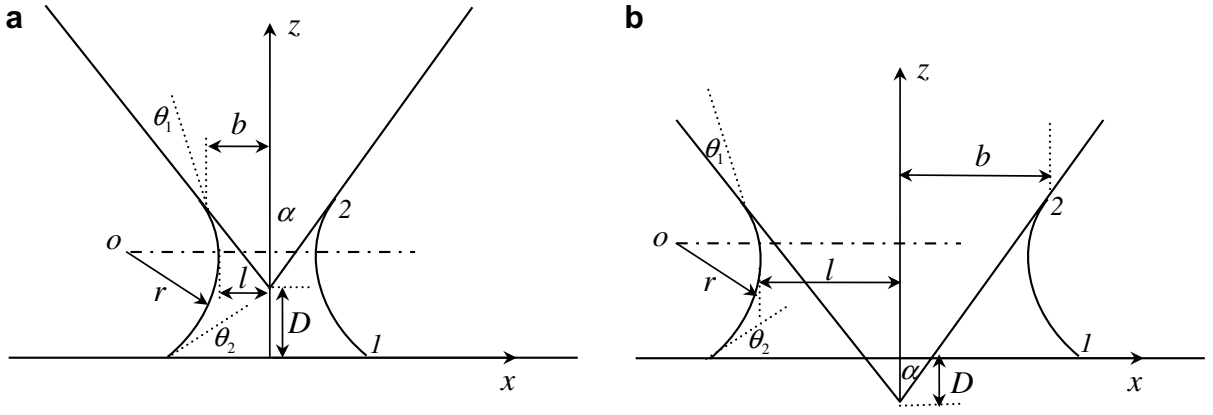

Fig. 1. Schematic illustration of a cone in wet adhesion with a substrate, the gap between them is D. (a) $D \geqslant 0$ and (b) $D < 0$.

$$\Delta p = \Delta\gamma\left(\frac{1}{l} - \frac{1}{r}\right) \tag{4}$$

where the two principal radii of curvature can be obtained from geometric relations,

$$r = \frac{[b/\tan\alpha + D]}{\sin(\alpha-\theta) + \cos\theta} \quad l = b - r[1 - \cos(\alpha - \theta)] \tag{5}$$

Substituting Eq. (4) into (3) yields

$$F_c = \pi b \Delta\gamma\left[2\cos(\alpha-\theta) + b\left(\frac{1}{r} - \frac{1}{l}\right)\right] \tag{6}$$

The volume of the liquid bridge V_l can be obtained as the volume of the figure yielded by rotating a circular arc of radius r about the y axis minus the volumes of the indenter immersed in the liquid V_s, that is

$$V_l = \int_{z_1}^{z_2} \pi x^2 \,\mathrm{d}z - V_s = \int_{z_1}^{z_2} \pi G^2(z)\mathrm{d}z - V_s \tag{7}$$

where the curve equation has the form

$$G(z) = r + l - \sqrt{r^2 - (z - r\cos\theta)^2} \tag{8}$$

and the coordinates of the contact points 1 and 2 as shown in Fig. 1 are

$$x_1 = r + l - r\sin\theta \quad x_2 = b \tag{9}$$

and

$$z_1 = 0 \quad z_2 = \frac{b}{\tan\alpha} + D \tag{10}$$

After derivation, the volume of the liquid bridge is written as

$$\begin{aligned} V_l = {} & \pi(z_2 - z_1)[(r+l)^2 + r^2] - \frac{\pi}{3}[(z_2 - r\cos\theta)^3 - (z_1 - r\cos\theta)^3] \\ & - 2\pi(r+l)\left[\frac{z - r\cos\theta}{2}\sqrt{r^2 - (z - r\cos\theta)^2} + \frac{r^2}{2}\arcsin\frac{z - r\cos\theta}{r}\right]\Bigg|_{z_1}^{z_2} - V_s \end{aligned} \tag{11}$$

The volume of V_s in Fig. 1a with $D \geqslant 0$ can be expressed as

$$V_s = \frac{\pi b^3}{3\tan\alpha} \tag{12}$$

(2) If $D < 0$ as shown in Fig. 1b, the capillary force can be written as

$$F_c = \pi\Delta\gamma\left(\frac{1}{r} - \frac{1}{l}\right)[b^2 - (D\tan\alpha)^2] + 2\pi b\Delta\gamma\cos(\alpha - \theta) \tag{13}$$

and the volume of the indenter immersed in the liquid is

$$V_s = \frac{\pi}{3}\left(\frac{b}{\tan\alpha} + D\right)[b^2 + (D\tan\alpha)^2 + b \mid D \mid \tan\alpha] \tag{14}$$

The formula of curvature radii of the liquid bridge, the coordinates of the contact points 1 and 2 are identical to Eqs. (5), (9) and (10), except that D has different sign.

4. Wet adhesion between a spherical indenter and a solid plane

The analysis model of a spherical indenter in wet adhesive contact with a substrate is shown in Fig. 2a, in which the distance between the substrate and the sphere is $D \geqslant 0$, ϕ is the filling angle, R is the radius of the

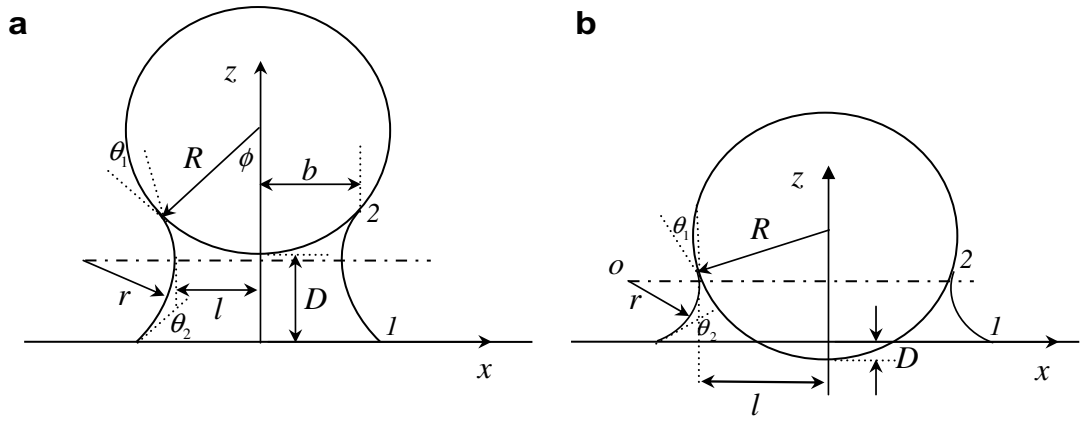

Fig. 2. Schematic illustration of a sphere in wet adhesion with a substrate, the gap between them is D. (a) $D \geqslant 0$ and (b) $D < 0$.

sphere, b is the radius of the circle of the liquid bridge wetting the sphere, $\theta_1 = \theta_2 = \theta$ is the contact angle, r and l are the curvature radii of the liquid bridge. Fig. 2b shows the corresponding model of $D < 0$.

The liquid pressure difference Δp inside and outside the meniscus is also expressed by the Young–Laplace equation (4), where the curvature radii of the liquid bridge are written as

$$r = \frac{R(1-\cos\phi)+D}{\cos(\theta+\phi)+\cos\theta} \tag{15}$$

and

$$l = r\sin(\theta+\phi) + R\sin\phi - r \tag{16}$$

(1) The capillary force F_c is the sum of the pressure difference and the axial component of the surface tension acting on the sphere. For the case of $D \geqslant 0$, the expression of the capillary force is

$$F_c = \pi R\sin\phi\Delta\gamma\left[2\sin(\theta+\phi) + R\sin\phi\left(\frac{1}{r}-\frac{1}{l}\right)\right] \tag{17}$$

The volume of the liquid bridge has the same form as that in Eq. (7), but the coordinates of contact points 1 and 2 as shown in Fig. 2a and b are,

$$x_1 = r + l - r\sin\theta, \quad x_2 = b = R\sin\phi \tag{18}$$

$$z_1 = 0, \quad z_2 = r\cos(\theta+\phi) + r\cos\theta \tag{19}$$

and the volume of the sphere immersed in the liquid is

$$V_s = \frac{\pi}{6}(R - R\cos\phi)[3(R\sin\phi)^2 + R^2(1-\cos\phi)^2] \tag{20}$$

(2) If $D < 0$, the capillary force F_c can be written as

$$F_c = -\pi\Delta p\{b^2 - [R^2 - (R+D)^2]\} + 2\pi b\Delta\gamma\sin(\theta+\phi) \tag{21}$$

and the volume of the sphere immersed in the liquid is

$$V_s = \frac{\pi}{6}(R - R\cos\phi + D)\{3b^2 + 3[R^2 - (R+D)^2] + (R - R\cos\phi + D)^2\} \tag{22}$$

The other formula are the same as those for $D \geqslant 0$.

5. Wet adhesion between a truncated conical indenter and a solid plane

In the micro- and nano-indentation experiments, the indenter tip is not actually ideal sharp due to the limitation of industry technology or tip wear after many times of experiments. The indenter tip is often repre-

sented by a spherical end. The capillary force between a truncated conical indenter and a substrate is studied in this section.

The truncated conical indenter is shown in Fig. 3, where R is the radius of the sphere, b is the radius of the circle of the liquid bridge wetting the truncated cone, $\phi_{\max}$ is half of the opening angle of the spherical part, α is half of the cone angle and D is the distance between the indenter and the substrate.

The formula of the capillary force and the volume of the immersed indenter are different for different indentation depths.

(1) First, we study the case of $D \geqslant 0$, i.e., the indenter does not penetrate into the substrate.

(1a) If $b < R\sin\phi_{\max}$, the contact point 2 lies on the sphere boundary, the liquid bridge forms between the spherical end and the substrate. All the formula are the same as those in Section 4 for $D \geqslant 0$.

(1b) If $b \geqslant R\sin\phi_{\max}$, the contact point 2 lies on the cone boundary. The curvature radii of the liquid bridge can be described as

$$r = \frac{\frac{b-R\sin\phi_{\max}}{\tan\alpha} + D + R(1-\cos\phi_{\max})}{\sin(\alpha-\theta)+\cos\theta} \tag{23}$$

$$l = r\cos(\alpha-\theta) + b - r \tag{24}$$

and the coordinates of contact points 1 and 2 in z direction are

$$z_1 = 0, \quad z_2 = r\sin(\alpha-\theta) + r\cos\theta \tag{25}$$

The capillary force in this case can be written as

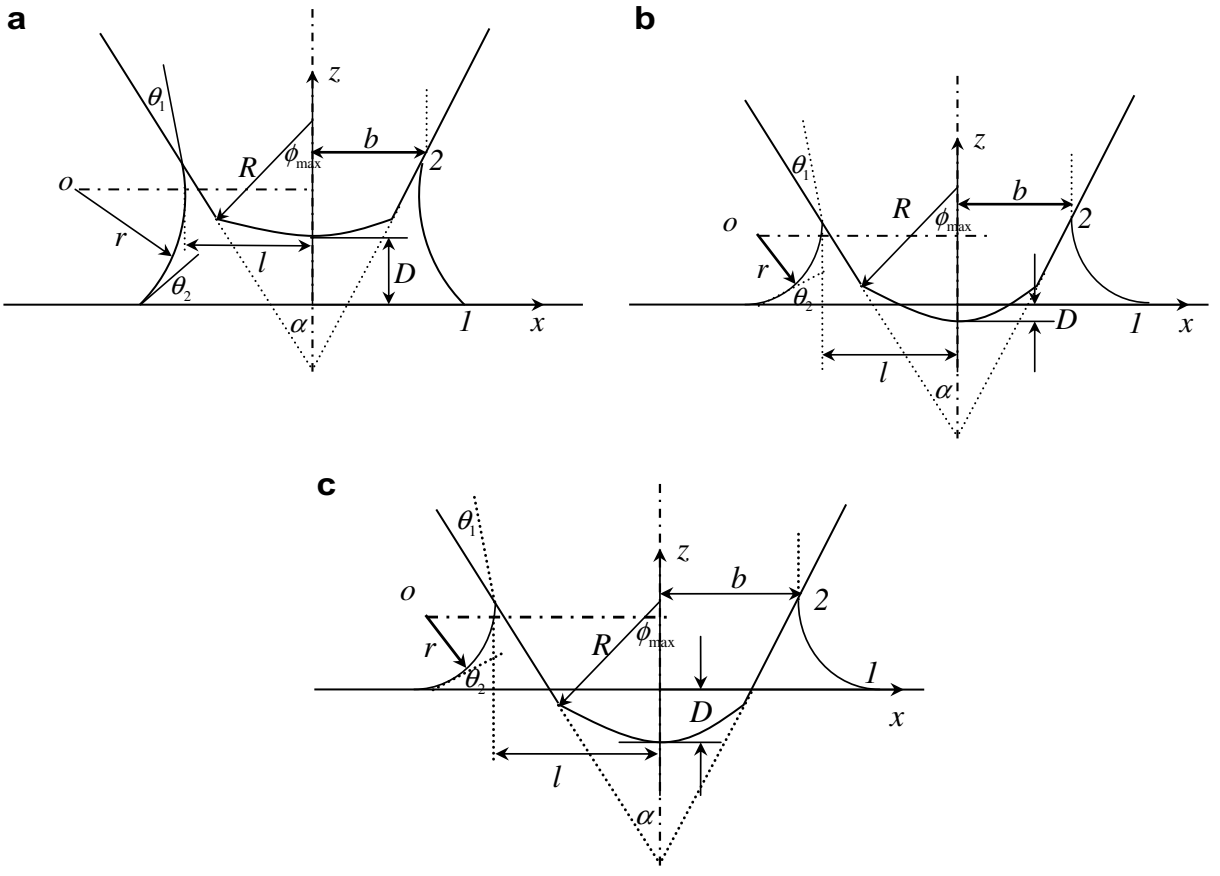

Fig. 3. Schematic illustration of a truncated cone with a spherical end in wet adhesion with a substrate, D is gap between them. (a) $D \geqslant 0$; (b) $D < 0$ and $|D| \leqslant R - R\cos\phi$; (c) $D < 0$ and $|D| > R - R\cos\phi_{\max}$.

$$F_c = \pi b \Delta\gamma \left[2\cos(\alpha - \theta) + b\left(\frac{1}{r} - \frac{1}{l}\right)\right] \tag{26}$$

where the Young–Laplace equation has been used.

The volume of the capillary liquid is still obtained as Eqs. (7) and (8), but the volume of the truncated conical indenter immersed in the liquid is

$$V_s = \frac{\pi}{3}R^3(1-\cos\phi_{\max})(1+\sin^2\phi_{\max}-\cos\phi_{\max}) + \frac{\pi}{3}h[(R\sin\phi_{\max})^2 + b^2 + bR\sin\phi_{\max}] \tag{27}$$

where

$$h = \frac{b - R\sin\phi_{\max}}{\tan\alpha} \tag{28}$$

(2) For the case of $D < 0$, two models as shown in Fig. 3b and c will be analyzed for $|D| \leqslant R - R\cos\phi_{\max}$ and $|D| > R - R\cos\phi_{\max}$, respectively.

(2a) $|D| \leqslant R - R\cos\phi_{\max}$ and $b \leqslant R\sin\phi_{\max}$. The liquid bridge forms between the spherical end and the substrate. All the formula describing the capillary force, the volume of the liquid bridge are the same as those in Section 4 for $D < 0$.

(2b) $|D| \leqslant R - R\cos\phi_{\max}$ and $b > R\sin\phi_{\max}$. The contact point 2 lies on the cone boundary as shown in Fig. 3b. The curvature radii of the liquid bridge can be written as

$$r = \frac{\frac{b - R\sin\phi_{\max}}{\tan\alpha} + D + R(1-\cos\phi_{\max})}{\sin(\alpha-\theta)+\cos\theta} \tag{29}$$

$$l = r\cos(\alpha-\theta) + b - r \tag{30}$$

and the coordinates of contact point 1 and 2 in z direction are

$$z_1 = 0, \quad z_2 = r\sin(\alpha-\theta) + r\cos\theta \tag{31}$$

Combining the two components, i.e., the pressure difference and the liquid surface tension acting in axial direction yields the capillary force,

$$F_c = -\pi\Delta p[b^2 - R^2 + (R+D)^2] + 2\pi b\Delta\gamma\cos(\alpha-\theta) \tag{32}$$

where Δp is expressed by the Young–Laplace equation.

The volume of the liquid bridge can also be expressed by Eq. (11), but the volume of the indenter immersed in the liquid consists of two parts

$$V_s = \frac{\pi}{3}\frac{b - R\sin\phi_{\max}}{\tan\alpha}[b^2 + (R\sin\phi_{\max})^2 + bR\sin\phi_{\max}] + \frac{\pi h}{6}[3(R\sin\phi_{\max})^2 + 3[R^2 - (R+D)^2] + h^2] \tag{33}$$

where the parameter h is

$$h = z_2 - \frac{b - R\sin\phi_{\max}}{\tan\alpha} \tag{34}$$

(2c) $|D| > R - R\cos\phi_{\max}$. In order to ensure the existence of the liquid bridge, $b > R\sin\phi_{\max} + [|D| - R(1-\cos\phi_{\max})]\tan\alpha$ is required. In this case, the curvature radii of the liquid bridge are

$$r\sin(\alpha-\theta) + r\cos\theta = \frac{b - R\sin\phi_{\max}}{\tan\alpha} + D + R(1-\cos\phi_{\max}) \tag{35}$$

and

$$l = r\cos(\alpha-\theta) + b - r \tag{36}$$

The coordinates of contact points 1 and 2 in z direction are

$$z_1 = 0 \quad z_2 = r\sin(\alpha-\theta) + r\cos\theta \tag{37}$$

The capillary force is

$$F_c = -\pi\Delta\gamma\left(\frac{1}{l}-\frac{1}{r}\right)\left[b^2-\left(\frac{b}{\tan\alpha}-z_2\right)^2\tan^2\alpha\right]+2\pi b\Delta\gamma\cos(\alpha-\theta) \tag{38}$$

and the volume of the liquid bridge can be described by Eqs. (7) and (8), but the volume of the indenter immersed in the liquid is

$$V_s = \frac{\pi z_2}{3}\left[b^2+\left(\frac{b}{\tan\alpha}-z_2\right)^2\tan^2\alpha+b\left(\frac{b}{\tan\alpha}-z_2\right)\tan\alpha\right] \tag{39}$$

6. Results and discussion

6.1. Numerical calculations

6.1.1. The case of a conical indenter and a substrate

From Eq. (5), one can see that for determined contact angle θ and cone angle 2α, if the radius of the circle of the liquid bridge wetting the cone b keeps unchanged, the curvature radius r will increase and l will decrease when the gap D between the cone and the substrate increases, then the capillary force F_c will decrease according to Eq. (6). If the gap D between the cone and the substrate keeps unchanged, then the capillary force will increase with an increasing radius of wetting circle b according to Eqs. (5) and (6). An example is shown in Fig. 4a. In order to be continuous, the results for $D<0$ according to Eqs. (5) and (13) are also included in Fig. 4a, from which one can see that the capillary force will increase when the indentation depth increases. The corresponding volumes of the liquid bridge can be obtained from Eqs. (11), (12) and (14), which are shown in Fig. 4b. Comparing Fig. 4a and b, one can see that if the contact angle, the cone angle and the radius of the wetting circle are fixed, the volume of the liquid bridge will decrease and the capillary force will increase when the indentation depth increases. This conclusion is only obtained from the mathematics point of view and has no physical meaning.

The contact angle embodies the features of hydrophobicity and hydrophilicity of objects. Fig. 5 shows the capillary force as a function of the contact angle θ when the cone angle α, the radius of the wetting circle b and the gap D between the cone and the substrate are unchanged. From Fig. 5, one can see that the capillary force decreases when the contact angle increases, i.e., the surfaces varying from hydrophilic to hydrophobic. With a fixed contact angle θ, the capillary force decreases when the gap between the cone and the substrate increases.

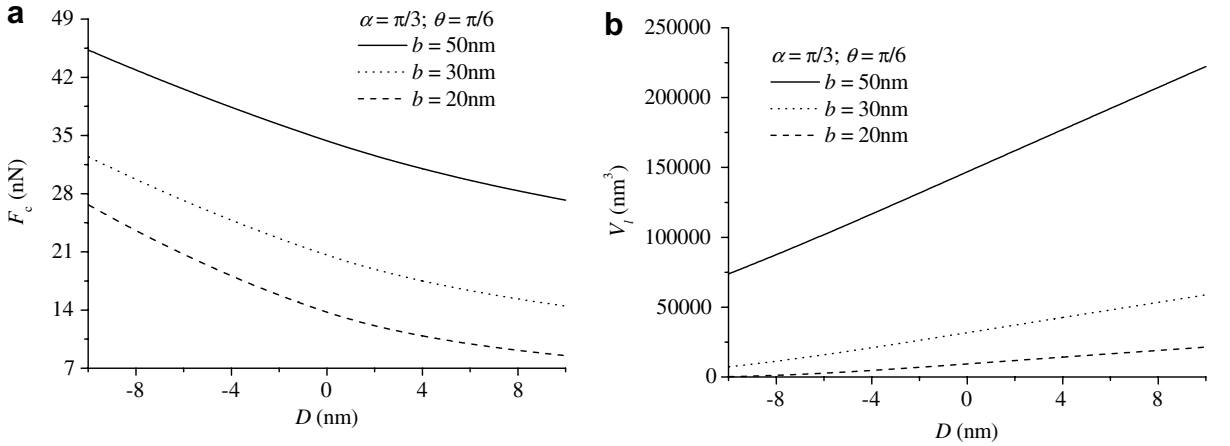

Fig. 4. (a) The capillary force F_c as a function of the gap D between the cone and the substrate for different values of b (the radius of the liquid bridge wetting the cones). (b) The volume of the liquid bridge as a function of the gap D between the cone and the substrate for different values of b (the radius of the liquid bridge wetting the cones).

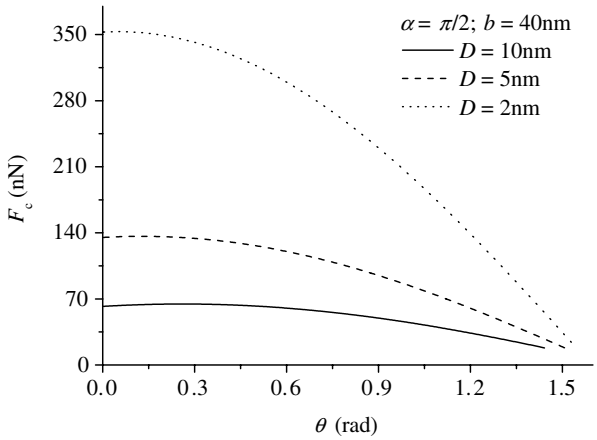

Fig. 5. The capillary force F_c as a function of the contact angle θ for different values of the gap D between the cone and the substrate.

With regard to the model of wet adhesion between a cone and a substrate shown in Fig. 1, it is convenient to use the radius of wetting circle b as a parameter. When the parameter b is varied, the values of the curvature radii r and l can be obtained as well as the relative humidity according to Eq. (2). Fig. 6a shows the capillary force as a function of the relative humidity, where one can see that the capillary force increases with humidity. The shape of the curve changes and the strength of the capillary force increases more quickly for a vanishing gap between the cone and substrate. For a fixed humidity, the capillary force increases with an increasing indentation depth. The capillary force in Fig. 6a is based on the Kelvin equation, which assumes a thermodynamic equilibrium of system. However, due to the speed of tip motion in small scale indenter, system with capillary condensed meniscus may not be governed by the Kelvin equation. In this case, constant meniscus volume has to be assumed. Fig. 6b shows the dependences of the capillary force on the volume of the liquid bridge for different gaps between the cone and substrate. One can see that the capillary force increases with the volume of the liquid bridge. Furthermore, one can find that, for a constant meniscus volume, the capillary force increases with an increasing indentation depth. The relation between the relative humidity and the meniscus volume is plotted in Fig. 6c, from which it is easy to find that the relative humidity increases with an increasing meniscus volume and tends to saturate when the volume attains about 10^{-22} m^3.

6.1.2. The case of a spherical indenter and a substrate

Using Eqs. (15)–(17), we plot the relations of the capillary force via the contact angle θ for the model of a spherical indenter in wet adhesion with a substrate as shown in Fig. 7, where one can see that the variation of the capillary force with the contact angle is different from that in the model of cone-plane. For a set of determined filling angle ϕ, gap D and radius of sphere R, there exists such a value of the contact angle that the capillary force attains maximum. For different spherical indenters with different radii and a fixed contact angle, one can find that the capillary force increases with the radius of the spherical indenter.

Using the resultant equations in Section 3, we can also determine the dependence of the capillary force on the volume of the liquid in the bridge. The variation of the capillary force via the volume of the liquid bridge is shown in Fig. 8a for different values of the distance between the indenter and the substrate. From Fig. 8a, one can see that the shape of the curves for $D > 0$ and $D \leqslant 0$ has large difference. In the case of $D \leqslant 0$, the capillary force is always decreasing with an increasing volume of the liquid bridge. In the case of $D > 0$, the capillary force increases, then decreases after attaining a maximum at a critical volume of the liquid bridge. If the meniscus volume is assumed to be a constant due to the speed of tip motion in small scale indenter, the changes in capillary force as a function of separation between the indenter and the sample are different for $D > 0$ from $D \leqslant 0$. In the case of $D > 0$, the capillary force decreases with an increasing separation. In the case of $D \leqslant 0$, the capillary force decreases with an increasing indentation depth. In the case of $D = 0$, i.e., point contact, the curvature radius r of the liquid bridge is much smaller than the curvature radius l when the meniscus volume tends to vanish, which results in qualitative difference for the results of $D = 0$ from those of $D > 0$.

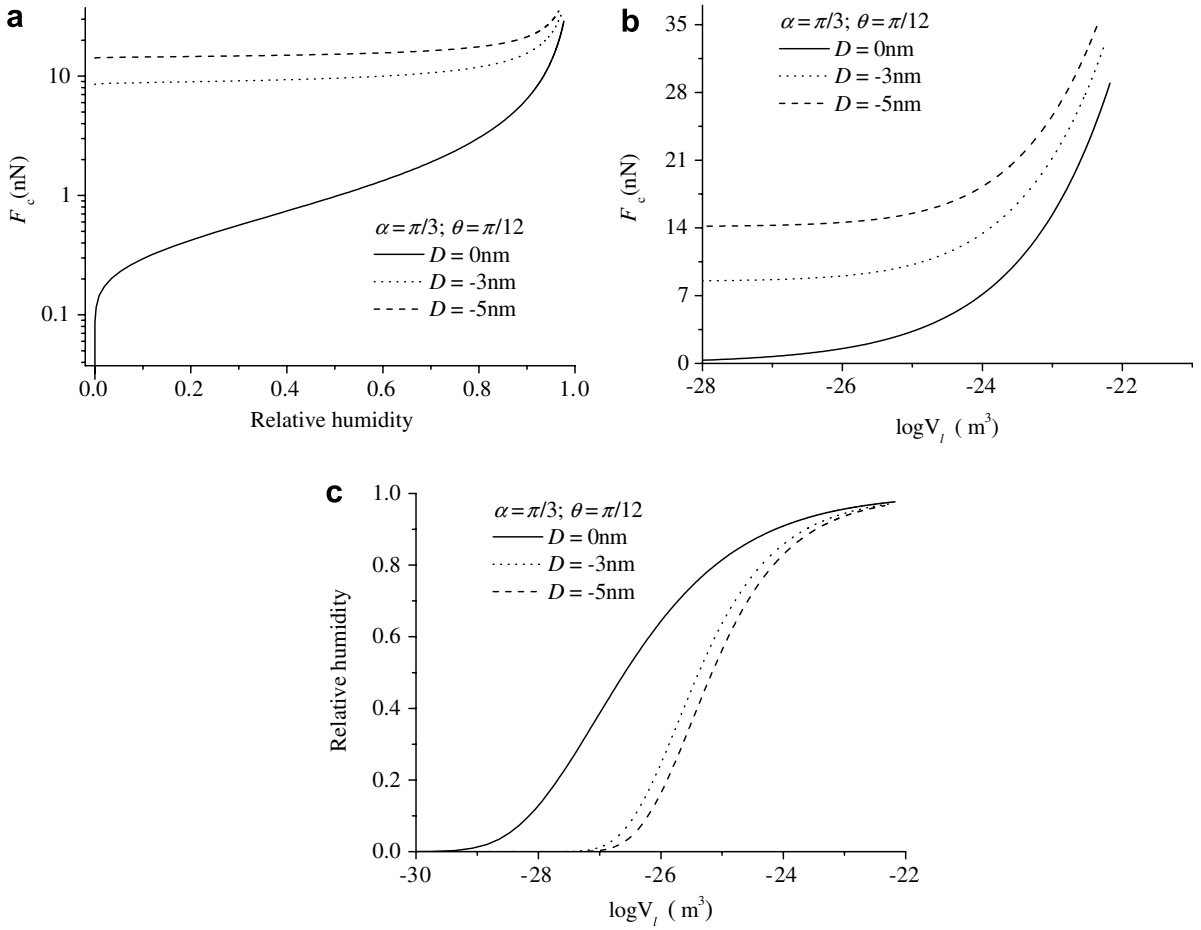

Fig. 6. (a) The capillary force F_c between a cone and a substrate versus humidity for different values of the gap D. (b) The dependence of the capillary force F_c on the volume of the liquid bridge for different values of gap D. (c) The dependence of the relative humidity on the meniscus volume for different values of gap D.

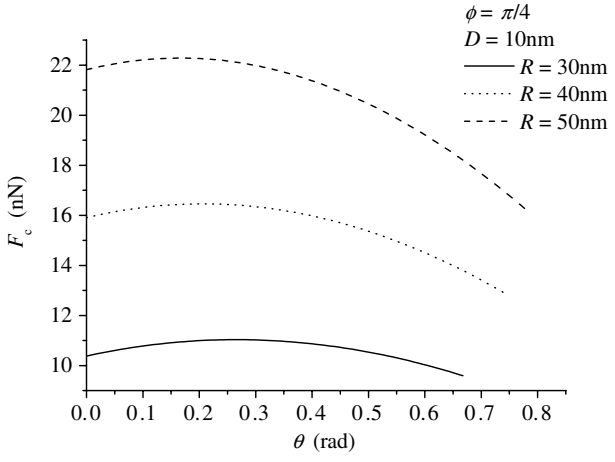

Fig. 7. The capillary force F_c as a function of the contact angle θ for different radii of the spherical indenter.

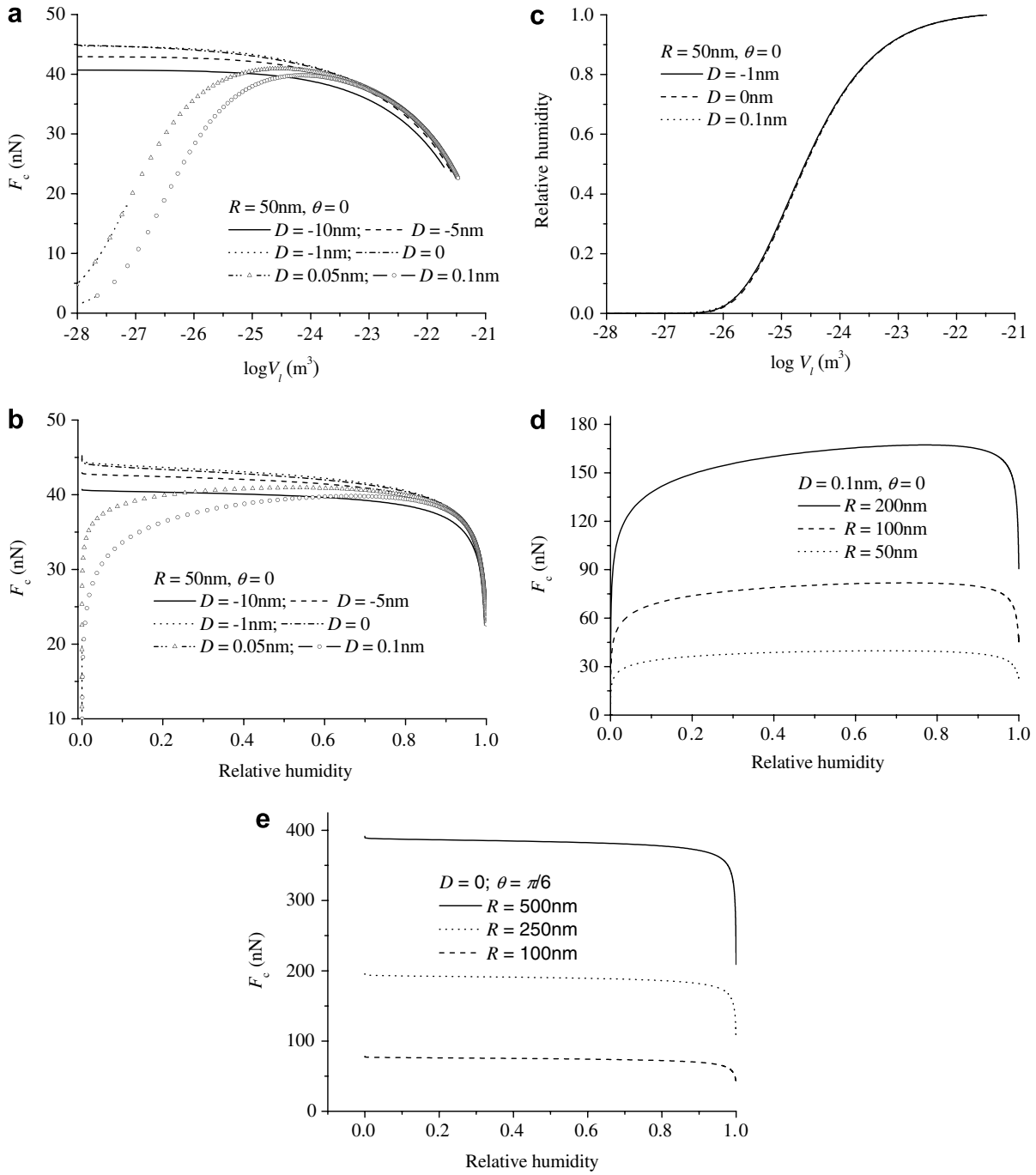

Fig. 8. (a) The capillary force F_c as a function of the volume of the liquid bridge for different gaps D between the spherical indenter and the substrate. (b) The capillary force F_c as a function of the humidity for different gaps between the spherical indenter and the substrate. (c) The dependence of the relative humidity on the meniscus volume for different values of D. (d) The capillary force F_c as a function of the humidity for different radii of the sphere and the gap between the sphere and the substrate is $D = 0.1$ nm. (e) The capillary force F_c as a function of the humidity for different radii of the sphere and vanishing gap between the sphere and the substrate.

An interesting phenomenon is also found in the relation between the capillary force and the relative humidity as shown in Fig. 8b, where we find that for the case of $D \leqslant 0$, the capillary force decreases very sharply at very small and very large humidity when the humidity increases, and keeps almost a constant at the moderate humid-

ity. Once the distance between the spherical indenter and the substrate deviate a very small value from zero and $D > 0$, the capillary force increases very sharply at smaller humidity and decreases very sharply at larger humidity when the humidity increases. The value of $D = 0$ becomes a critical one for the relation between the capillary force and the relative humidity. The effect of the van der Waals force at small humidity has been discussed by Farshchi-Tabrizi et al. (2006). The relation between the meniscus volume and the relative humidity is shown in Fig. 8c in order to give a more clear understanding, from which one can see that the relative humidity increases when the meniscus volume increases, and at a critical value of the volume the relative humidity saturates.

Fig. 8d and e shows the relation between the capillary force and the relative humidity for the case of spherical indenter with different radii. The capillary force increases when the radius of the spherical indenter increases, which is consistent well with the numerical results in Pakarinen et al. (2005).

The effect of contact angle on the capillary force is shown in Fig. 9, where it is easy to find that the capillary force decreases with increasing contact angle, i.e., if the surfaces become hydrophobic from hydrophilic, the capillary force will decrease.

6.1.3. The case of a truncated conical indenter and a substrate

Fig. 10 shows the relation between the capillary force and the volume of the liquid bridge for the model of a truncated cone with a spherical end in wet adhesion with a substrate, in which the gap D between the truncated cone and the substrate, the opening angle of the spherical end, the cone angle and the contact angle are fixed,

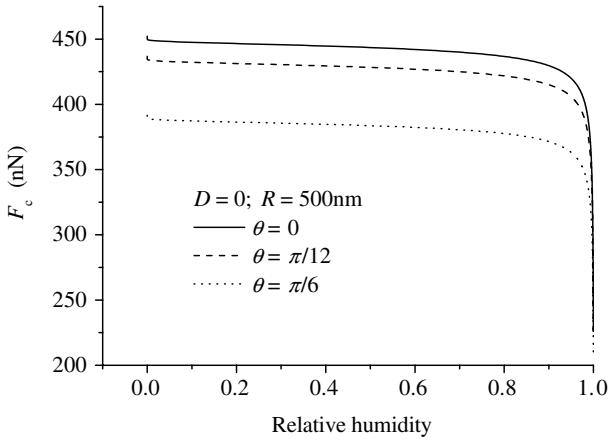

Fig. 9. The capillary force F_c between a sphere and a substrate versus humidity for different contact angles θ.

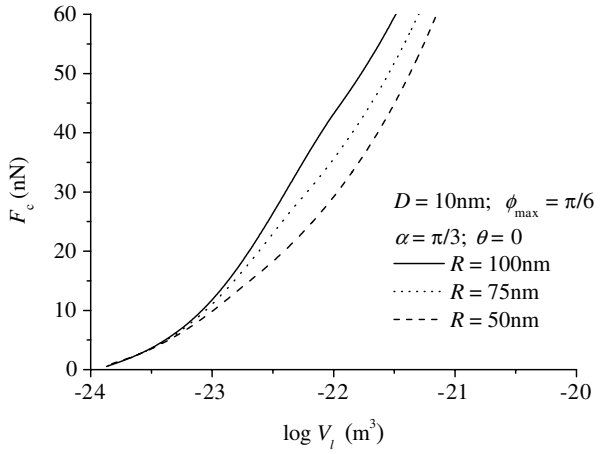

Fig. 10. The dependence of the capillary force F_c between a truncated cone and a substrate on the volume of the liquid bridge for different radii of the spherical end.

except for the radius of the spherical end. One can see that for a determined radius of the spherical end, the capillary force increases with an increasing volume of the liquid bridge. If the volume of the liquid bridge keeps a small constant, the capillary force increases with a decreasing radius of the spherical end. For a large constant of the volume of the liquid bridge, the case is on the contrary.

The effect of the contact angle on the capillary force is shown in Fig. 11, where all the parameters are fixed except for the contact angle. One can see the capillary force increases at small contact angle, then decreases after a critical value of the contact angle, at which the capillary force attains maximum value. Fig. 11 also shows that the capillary force increases with a decreasing gap between the truncated end and the substrate if all the other parameters keep unchanged.

The capillary force versus the relative humidity is shown in Fig. 12, in which we consider tips with smooth ($\alpha + \phi_{\max} = 90°$) and non-smooth ($\alpha + \phi_{\max} \neq 90°$) transitions between the spherical and conical parts and two cases of $D = 0$ and $D \neq 0$. For the case of $D \neq 0$, one can see that the capillary force increases with the relative humidity up to a relatively high humidity for the case of a smooth transition, the spherical end dominates the capillary force. The conical part is only important at very high humidity. For the case of a non-smooth transition, the relation between the capillary force and the relative humidity consists of three regimes along with an increasing relative humidity: (i) the capillary force increases at the initial stage, (ii)

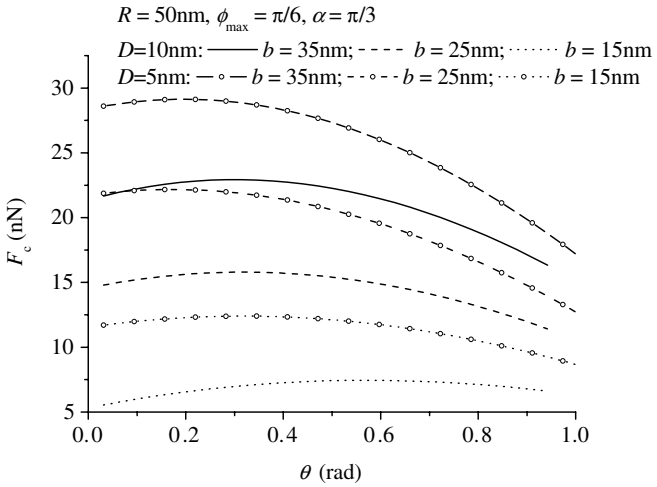

Fig. 11. The dependence of the capillary force F_c between a truncated cone and a substrate on the contact angles θ for different gaps D and different radii b of the liquid bridge wetting the truncated cone.

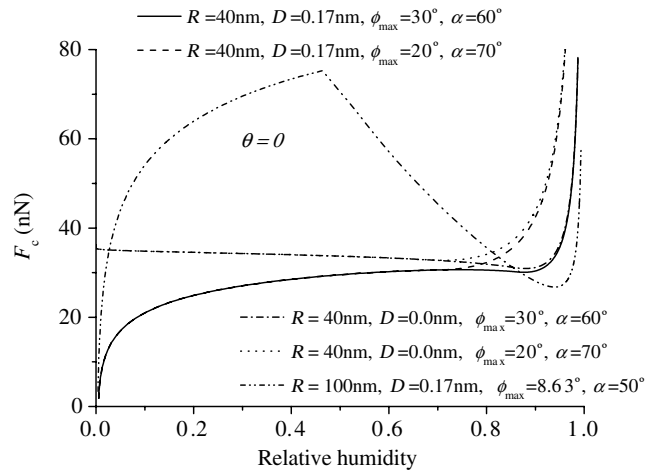

Fig. 12. The capillary force F_c between a truncated cone and a substrate as a function of the humidity for different sets of parameters.

decreases at certain value of the relative humidity, and (iii) then increases once again. The three regimes correspond to the dominations of spherical end, intermediate transition and conical part, respectively. For the case of $D = 0$, the capillary force keeps almost a constant up to a relatively high humidity when the spherical end dominates the capillary force, the conical part is only important at very high humidity also.

When a truncated conical indenter penetrates a depth into the substrate, the relation between the capillary force and the relative humidity is shown in Fig. 13. The capillary force decreases up to a relatively high humidity, then increases, which means the spherical end dominates up to a relatively high humidity, then the conical part plays an important role. For a smooth transition between the spherical and conical parts, the curves of the relation between the capillary and humidity have smooth transitions also; For a non-smooth transition of the shape of a truncated indenter, the corresponding curves have a sharp transition between the regime of spherical part domination and that of conical part domination.

If the indent depth increases continuously, the relations between the capillary force and the indent depth are shown in Fig. 14a–c, in which the effects of the contact angle, the radius of the spherical end, the relative humidity are considered, respectively. From the three figures, one can see that the curves of the capillary force via the indenting depth consists of four regimes for the case of non-smooth transition between the spherical and conical parts of indenter, and three regimes for the case of smooth transition as shown in Fig. 15. In the case of non-smooth transition, when $D < 0$, the capillary is in turn dominated by the spherical part, intermediate transition part and the conical part along with an increasing indent depth. In the case of smooth transition, when $D < 0$, it is only dominated in turn by the spherical and conical parts. In these two cases with $D < 0$, the capillary force is always decreasing with an increasing indent depth in the regime dominated by the spherical part and in the other regimes always increasing with an increasing indent depth. When $D > 0$, the capillary force is always decreasing with an increasing gap D. For a determined contact angle or a relative humidity, the capillary force is significantly influenced by the indent depth as shown in Fig. 14a and c.

6.2. The effect of capillary force on the indentation hardness

In micro- and nano-indentation experiments, an external load is added on the indenter and normal to the indented surface which is compressed to form an indentation. We define the external force as F_n, which is measured by the indentation instrument spontaneously. If the capillary force F_c is attractive, the indented depth is amplified as well as the contact area A in the experiment, which is also measured by the indentation instrument automatically. The definition of the hardness

$$H = \frac{F_n}{A} \tag{40}$$

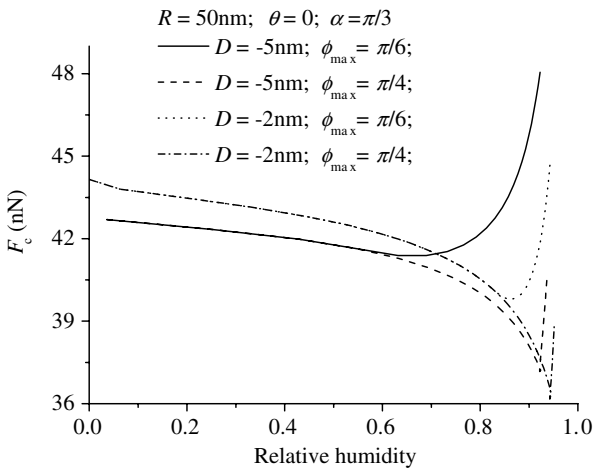

Fig. 13. The capillary force F_c between a truncated cone and a substrate as a function of the humidity for different gaps D and half of the opening angle ϕ_{max} of the spherical end.

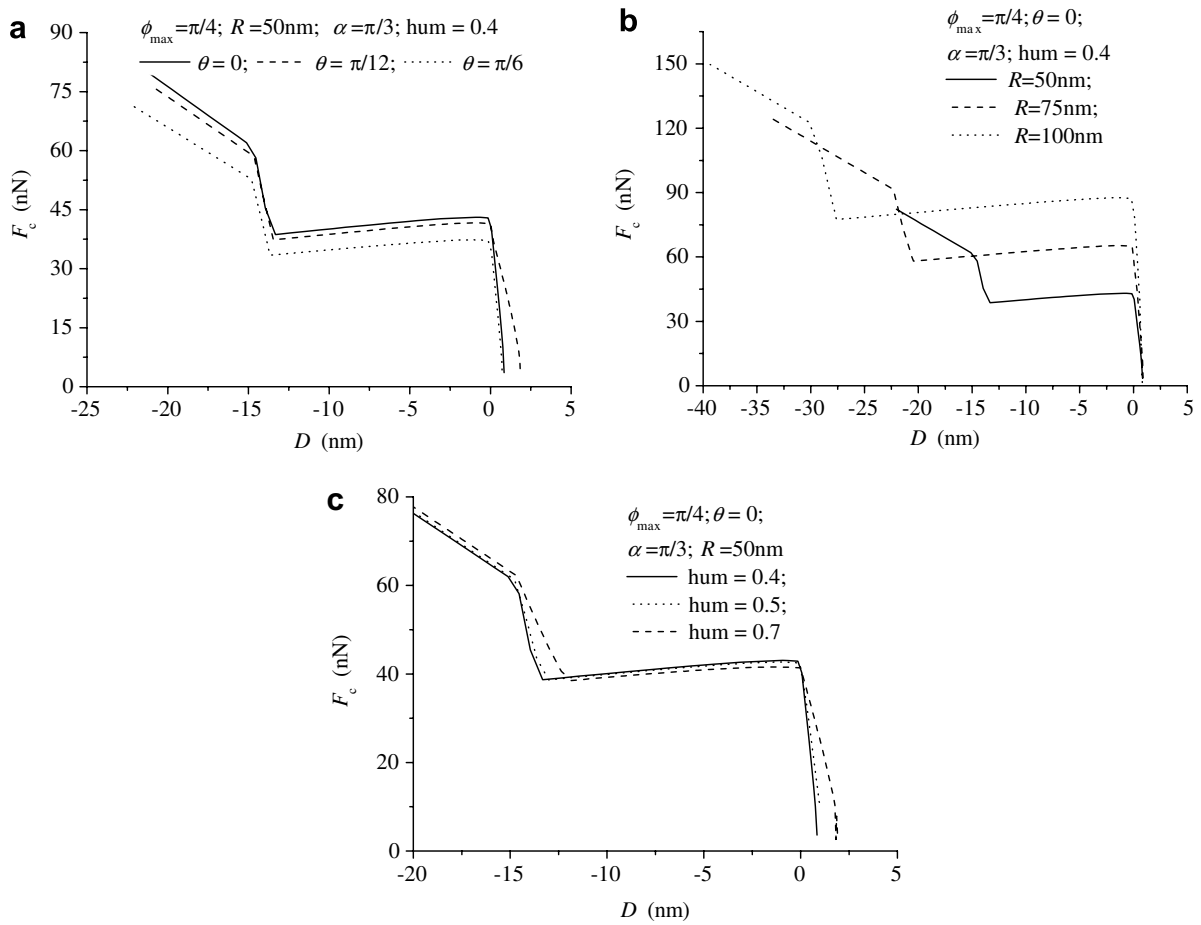

Fig. 14. The capillary force F_c between a truncated cone and a substrate as a function of the gap D: (a) for different contact angles θ; (b) for different radii of the spherical end; (c) for different humidity.

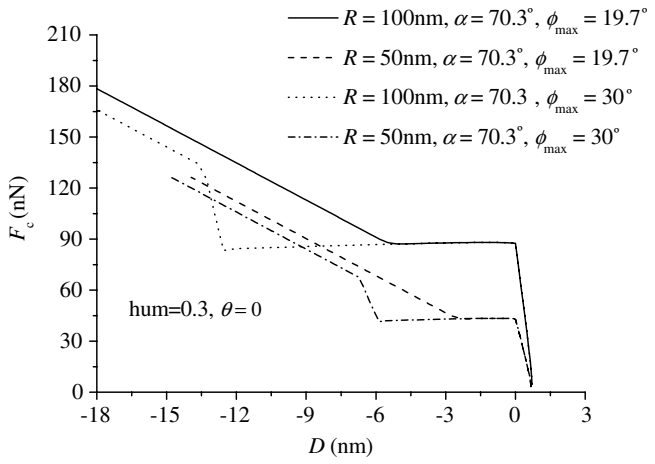

Fig. 15. The dependence of the capillary F_c between a conical indenter with a rounded tip and a substrate on the gap D between the indenter and the substrate for different sets of radii R and half of the opening angle ϕ_{max} of the rounded tip.

leads to an underestimation due to the overestimated contact area A. On the other hand, the measured hardness should be overestimated if the capillary force is repulsive.

For convenience, the commonly used Berkovich indenter in the indentation experiments is usually approximated to be a cone with half of the cone angle $\alpha = 70.3°$ in the FEM simulations. Due to the cone wear, the tip is rounded with a radius about $R = 50$–100 nm. The capillary force is plotted in Fig. 15 for different radii of rounded tips and different opening angles for different transitions between the spherical and conical parts, from which one can see the capillary force is always attractive during the indentation process and influenced by the radius R and opening angle $\phi_{\max}$ significantly. The capillary force increases with an increasing radius of the rounded tip. The dominated regime by the spherical end increases with the opening angle. Conclusion can be made that the measured hardness should be underestimated due to the effect of the capillary force, so that the "size effect" in the micro- or nano-experiments is not due to the influence of the capillary force but the other factors.

Acknowledgements

S.C. thanks the support by NSFC (10672165, 10732050, 10721202) and KJCX2-YW-M04.

References

Autumn, K., Sitti, M., Liang, Y.C., Peattie, A.M., Hansen, W.R., Sponberg, S., Kenny, T.W., Fearing, R., Israelachvili, J.N., Full, R.J., 2002. Evidence for van der Waals adhesion in gecko setae. Proc. Natl. Acad. Sci. USA 99, 12252–12256.

Chen, S.H., Liu, L., Wang, T.C., 2004a. Strain gradient effects in nanoindentation of film-substrate systems. Acta Mater. 52 (5), 1089–1095.

Chen, S.H., Tao, C.J., Wang, T.C., 2004b. A study of micro-indentation with size effects. Acta Mech. 167 (1–2), 57–71.

Dixon, A.F.G., Croghan, P.C., Gowing, R.P., 1990. The mechanism by which aphids adhere to smooth surfaces. J. Exp. Biol. 152, 243–253.

Eisner, T., Aneshansley, D.J., 2000. Defense by foot adhesion in a beetle (*Hemisphaerota cyanea*). Proc. Natl. Acad. Sci. USA 97, 6568–6573.

Farshchi-Tabrizi, M., Kappl, M., Cheng, Y., Gutmann, J., Butt, H., 2006. On the adhesion between fine particles and nanocontacts: an atomic force microscope study. Langmuir 22, 2171–2184.

Federle, W., Baumgartner, W., Holldobler, B., 2004. Biomechanics of ant adhesive pads: frictional forces are rate- and temperature-dependent. J. Exp. Biol. 206, 67–74.

Fortes, M.A., 1982. Axisymmetric liquid bridges between parallel plates. J. Colloid Interface Sci. 88, 338–352.

Huang, Y., Xue, Z., Gao, H., Nix, W.D., Xia, Z.C., 2000. A study of micro-indentation hardness tests by mechanism-based strain gradient plasticity. J. Mater. Res. 15, 1786–1796.

Kesel, A.B., Martin, A., Seidl, T., 2003. Adhesion measurements on the attachment devices of the jumping spider *Evarcha arcuata*. J. Exp. Biol. 206, 2733–2738.

Maboudian, R., 1998a. Surface processes in MEMS technology. Surf. Sci. Rep. 30, 207–269.

Maboudian, R., 1998b. Adhesion and friction issues associated with reliable operation of MEMS. MRS Bull. 23, 47–51.

Maboudian, R., Howe, R.T., 1997. Critical review: adhesion in surface micromechanical structures. J. Vac. Sci. Technol. B 15 (1), 1–20.

Maboudian, R., Ashurst, W.R., Carraro, C., 2000. Self-assembled monolayers as anti-stiction coatings for MEMS. Sen. Actuators A 82, 219–223.

Ma, Q., Clarke, D.R., 1995. Size dependent hardness in silver single crystals. J. Mater. Res. 10, 853–863.

McElhaney, K.W., Vlassak, J.J., Nix, W.D., 1998. Determination of indenter tip geometry and indentation contact area for depth-sensing indentation experiments. J. Mater. Res. 13, 1300–1306.

Nix, W.D., Gao, H., 1998. Indentation size effects in crystalline materials: a law for strain gradient plasticity. J. Mech. Phys. Solids 46, 411–425.

Obata, K.J., Motokado, T., Saito, S., Takahashi, K., 2004. A scheme for micro-manipulation based on capillary force. J. Fluid Mech. 498, 113–121.

Orr, F.M., Scriven, L.E., Rivas, A.P., 1975. Pendular rings between solids: meniscus properties and capillary force. J. Fluid Mech. 67, 723–742.

Pakarinen, O.H., Foster, A.S., Paajanen, M., et al., 2005. Towards an accurate description of the capillary force in nanoparticle–surface interactions. Model. Simul. Mater. Sci. Eng. 13, 1175–1186.

Qian, J., Gao, H., 2006. Scaling effects of wet adhesion in biological attachment systems. Acta Biomater. 2, 51–58.

Tanikawa, T., Hashimoto, Y., Arai, T., 1998. Micro drops for adhesive bonding of micro assemblies and making a 3-d structure "micro scarecrow". Proc. IEEE Intl Conf. on Intelligent Robots and Systems, 776–781.

Tselishchev, Y.G., Val'tsifer, V.A., 2003. Influence of the type of contact between particles joined by a liquid bridge on the capillary cohesive forces. Colloid J. 65, 385–389.

Yoon, E., Yang, S.H., Han, H., Kong, H., 2003. An experimental study on the adhesion at a nano-contact. Wear 254, 974–980.